



# VCU

Virginia Commonwealth University  
VCU Scholars Compass

---

Theses and Dissertations

Graduate School

---

2021

## Pushing the limits: Increasing the speed and specificity of SARS-CoV-2 testing

Grayson Way

Follow this and additional works at: <https://scholarscompass.vcu.edu/etd>



Part of the [Diagnosis Commons](#), and the [Immunology and Infectious Disease Commons](#)

© The Author

---

Downloaded from

<https://scholarscompass.vcu.edu/etd/6600>

This Thesis is brought to you for free and open access by the Graduate School at VCU Scholars Compass. It has been accepted for inclusion in Theses and Dissertations by an authorized administrator of VCU Scholars Compass. For more information, please contact [libcompass@vcu.edu](mailto:libcompass@vcu.edu).

© Grayson W. Way 2021

All Rights Reserved

Pushing the limits: Increasing the speed and specificity of SARS-CoV-2 testing

A thesis submitted in partial fulfillment of the requirements for the degree of Master of  
Science at Virginia Commonwealth University

By

Grayson Welch Way

B.S., James Madison University 2011

Director: Rebecca K. Martin, PhD

Assistant Professor

Department of Microbiology and Immunology

School of Medicine

Virginia Commonwealth University

Richmond, VA

## Acknowledgements

I would like to thank my advisor and mentor Rebecca Martin, PhD. She encouraged me to think critically and was always supportive and confident in my abilities even when I was not. Her passion for science and leadership will continue to motivate me in the future. This work would not have been possible without her and I truly cannot thank her enough.

I would also like to thank the past and present Martin lab members: Matthew Zellner, Anuj Tharakan, Joseph Lownik, Jared S. Farrar, Stephanie Duong, T.J. Smith, Jr., and Andrea Luker. It truly was a work family and a joy to be a part of the team. Their help throughout the academic and research process has been indispensable.

I also would like to thank my graduate committee members John Ryan, PhD and Joyce Lloyd, PhD for their guidance and support.

Finally, I would like to thank my family for their love and support.

## Table of Contents

Acknowledgements.....	iii
List of Figures .....	v
List of Abbreviations.....	vi
Abstract .....	viii
Introduction .....	1
COVID-19.....	1
Current methods for testing of infectious diseases.....	6
Polymerase Chain Reaction (PCR).....	9
Polymerase Improvements.....	11
The evolution of PCR (Hot start PCR, RT-PCR, qRT-PCR, extreme PCR).....	13
Materials and Methods.....	16
Specimen acquirement and storage .....	16
Primers.....	17
Reagents.....	18
Mastermixes .....	18
Melt curve analysis .....	19
PCR Thermocycling conditions.....	19
RT optimization.....	21
PCR cycle time optimization .....	22
Results.....	22
RT optimization.....	22
PCR cycle optimization.....	24
Direct Light Cyclers Validation.....	28
Extreme RT-PCR for SARS-CoV-2.....	30
Discussion .....	32
References .....	35

## List of Figures

Figure 1. SARS-CoV-2 structure and common symptoms. ....	2
Figure 2. SARS-CoV-2 Spike protein. ....	3
Figure 3. ACE2 tissue expression. ....	5
Figure 4. Infectious disease testing methods. ....	7
Figure 5. CDC COVID-19 N1-RnaseP probe-based qRT-PCR assay. ....	9
Figure 6. Polymerase Chain Reaction - PCR basic steps. ....	10
Figure 7. Fluorescent Probe-based Real Time PCR (qRT-PCR). ....	14
Figure 8. Extreme PCR vs Conventional PCR ....	15
Figure 9. SARS-CoV-2 testing procedure schematic. ....	20
Figure 10. Extreme PCR setup ....	21
Figure 11. Reverse Transcription Optimization:.....	24
Figure 12. PCR cycle time optimization:.....	27
Figure 13. Direct Light Cycler validation:.....	29
Figure 14. Extreme RT-PCR for SARS-CoV-2:.....	31

## List of Abbreviations

2019-nCoV	2019 novel coronavirus
BHQ1	Black Hole Quencher 1
CDC	Centers for Disease Control and Prevention
COVID-19	Coronavirus disease 2019
DNA	Deoxyribonucleic acid
dsDNA	double stranded DNA
ssDNA	single stranded DNA
dNTP	Deoxynucleotide triphosphate
ELISA	Enzyme-linked immunosorbent assay
FAM	6-carboxyfluorescein
K <sub>m</sub>	Michaelis Constant
MERS-CoV	Middle East respiratory syndrome coronavirus
nCoV-19	novel coronavirus 2019
Nsp1	Nonstructural protein 1
ORFs	open reading frames
PCR	Polymerase Chain Reaction

qRT-PCR	Quantitative real-time PCR
RT-PCR	Reverse-transcription PCR
RNA	Ribonucleic acid
RT	Reverse Transcriptase
[S]	Substrate concentration
SARS-CoV	Severe acute respiratory syndrome
SARS-CoV-2	Severe acute respiratory syndrome coronavirus 2
TMPRSS2	transmembrane protease serine 2
UTM	Universal Transport Media
VTM	Viral Transport Media
$v$	enzymatic velocity



## Abstract

### PUSHING THE LIMITS: INCREASING THE SPEED AND SPECIFICITY OF SARS-COV-2 TESTING

Grayson Welch Way

B.S., James Madison University, 2011

A thesis submitted in partial fulfilment of the requirements for the degree of Master of Science at Virginia Commonwealth University

Virginia Commonwealth University 2021

Director: Rebecca K. Martin, PhD

Assistant Professor

Department of Microbiology and Immunology

School of Medicine

The prevalence and spread of the current COVID-19 pandemic have highlighted the importance of continual improvements upon current microbiological testing methods. Rapid and accurate testing can help mitigate spread by improving on the time to quarantine and quarantine duration required. As of the writing of this thesis, COVID-19 has been responsible for more than 500,000 deaths in the United States of America, and greater than 2 million deaths globally. The work done in this thesis has shown improvements in the current SARS-CoV-2 testing methodology by reducing the time it takes for patient testing while maintaining accuracy and the sensitivity required of a clinical assay. The protocol developed uses extraction-free RT-PCR testing as well as a rapid RT-PCR methodology. The assay can improve speed and maintain its specificity using probe-based detection for the SARS-CoV-2 N gene. This research provides a template for increasing the speed of testing for SAR-CoV-2 that can be applied to other infectious diseases and thereby help reduce the spread of future epidemics and pandemics.

## Introduction

### COVID-19

Severe acute respiratory syndrome coronavirus 2 (SARS-CoV-2), previously nCoV-19 or 2019-nCoV, is the causative agent responsible for the current coronavirus disease (COVID-19) pandemic that has been unfolding for over a year now<sup>5, 9, 55</sup>. As of January 17<sup>th</sup>, 2021, according to the “COVID-19 Dashboard by the Center for Systems Science and Engineering (CSSE) at Johns Hopkins University (JHU),” COVID-19 has infected over 93 million people globally and has resulted in just over 2 million deaths<sup>9</sup>. In the United States alone, there have been over 23 million cases resulting in nearly 400,000 deaths<sup>9</sup>. SARS-CoV-2 is a coronavirus, so named for the large spike proteins that cause the viral shape to resemble a crown. Coronaviruses are in the family *Coronaviridae* in the suborder *Cornidovirinae* and infect a range of different animals. They have had a history of causing mild to severe respiratory infections in humans. There have been two previous zoonotic coronavirus outbreaks prior to this current pandemic. In 2002 there was an outbreak of severe acute respiratory syndrome coronavirus (SARS-CoV) in China, and in 2012 there was an outbreak of the Middle East respiratory syndrome coronavirus (MERS-CoV), both causing fatal respiratory infections<sup>7, 15</sup>. The basic SARS-CoV-2 structure, components and symptoms caused can be visualized in Figure 1.

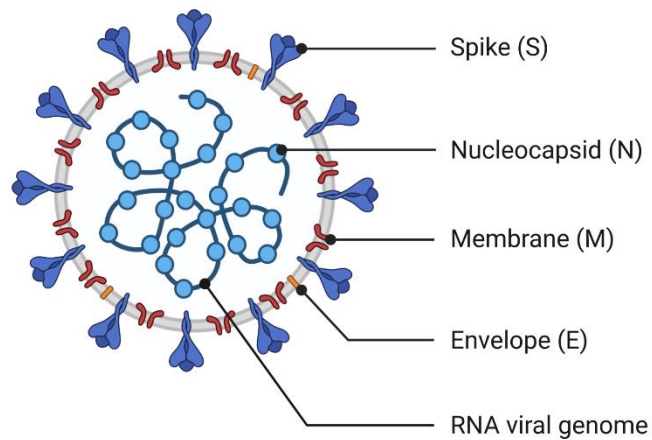
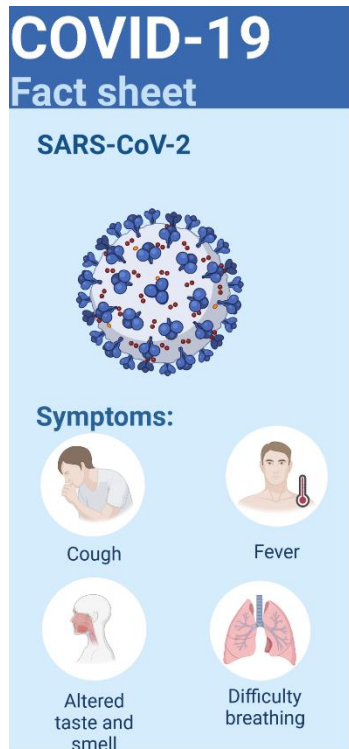


Figure 1. SARS-CoV-2 structure and common symptoms. <sup>1</sup>

SARS-CoV-2 is further classified as a  $\beta$ -coronavirus (one of four genera of coronaviruses).  $\beta$ -coronaviruses are enveloped, positive-sense RNA viruses that infect mammals. SARS-CoV-2 shares 50% and 79% sequence homology with MERS-CoV and SARS-CoV respectively<sup>29</sup>. It has 88% sequence homology to two bat SARS-like coronaviruses (bat-SL-CoVZC45 and bat-SL-CoVZXC21)<sup>29</sup>. The pandemic is believed to have originated as a zoonosis from bats in Wuhan, China where it was first reported<sup>29</sup>. SARS-CoV-2 contains six functional open reading frames (ORFs), arranged in a 5' to 3' <sup>22</sup>order that encode for: replicase polyprotein (ORF1a/ORF1b), spike (S) glycoprotein, envelope (E), membrane (M), and nucleocapsid (N) proteins; there are

<sup>1</sup> Figure Created with BioRender.com

also several nonstructural proteins and interspersed putative ORFs<sup>15</sup>. Of the nonstructural proteins, nonstructural protein 1 (Nsp1) has been shown to play a major role in SARS-CoV-2 virulence by suppressing host gene expression<sup>50</sup>. There have been several new strains to arise and the COVID-19 pandemic has shown increasing heterogeneity<sup>15, 17, 29, 36</sup>. The iconic spike protein is provides the mechanism by which SARS-CoV-2 invades host cells, via interaction with angiotensin converting enzyme 2 (ACE2), similar to SARS-CoV<sup>8, 15, 54</sup>. The spike protein structure is shown in Figure 2.

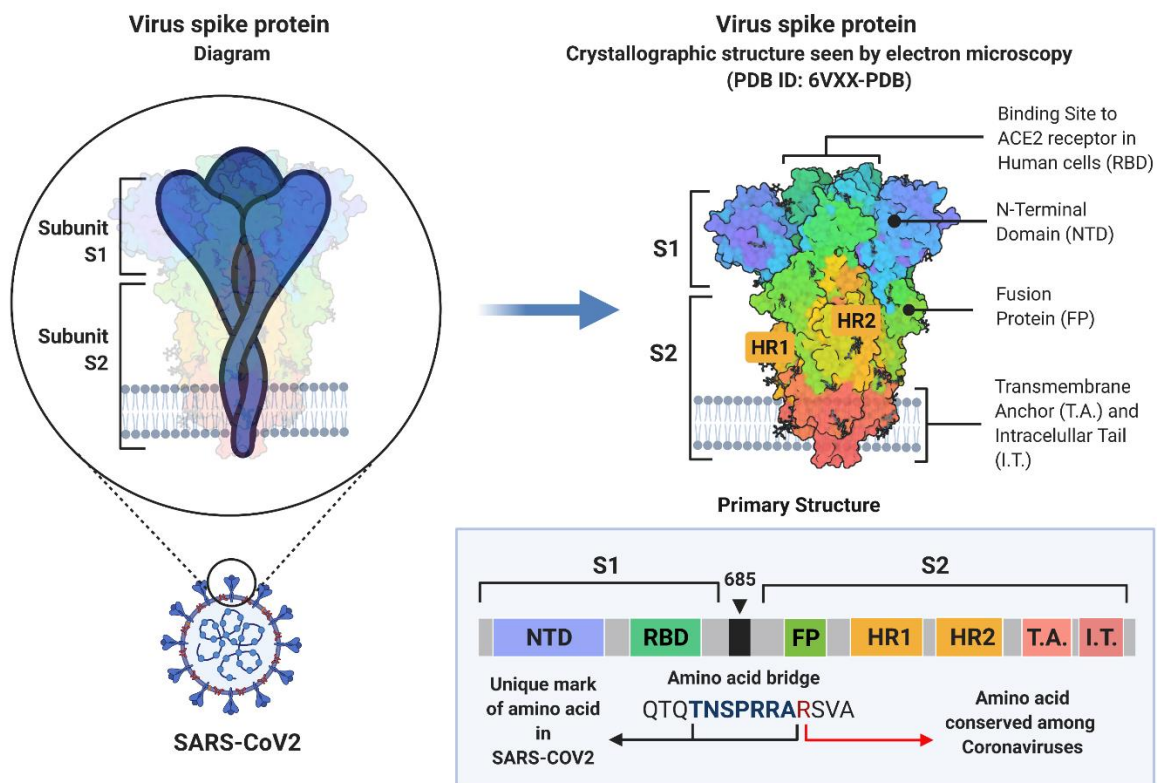


Figure 2. SARS-CoV-2 Spike protein.<sup>2</sup>

<sup>2</sup> Figure Created with BioRender.com

Upon binding to ACE2, the host transmembrane protease serine 2 (TMPRSS2) cleaves the spike protein, activating it<sup>14</sup>. After cleavage of the spike protein, SARS-CoV-2 enters the cell by endocytosis, or by fusion of the viral and host membranes<sup>56</sup>. Once SARS-CoV2 enters the host cell, it releases its positive-sense RNA genome into the cytosol, where host ribosomes can directly translate the early viral proteins, which are predominantly viral replicative particles<sup>41</sup>. Nsp1 plays a role in aiding SARS-CoV-2 replication by binding the 40s ribosomal subunit similar to Nsp1 of SARS-CoV<sup>16, 50</sup>. This binding to the ribosome inhibits the translation of host mRNAs but still allows translation of viral RNAs<sup>16, 50</sup>. The exact mechanism for how viral RNAs are still allowed to be translated is still unknown but it is believed that there is an interaction with the 5' cap of the viral RNAs and Nsp1 that allows translation to continue<sup>16, 50</sup>. Much of the site associated damage and patient symptoms seen in COVID-19 infection can be explained by observation of tissue specific ACE2 expression, seen in Figure 3.

## Host Tissues Known to Express ACE2

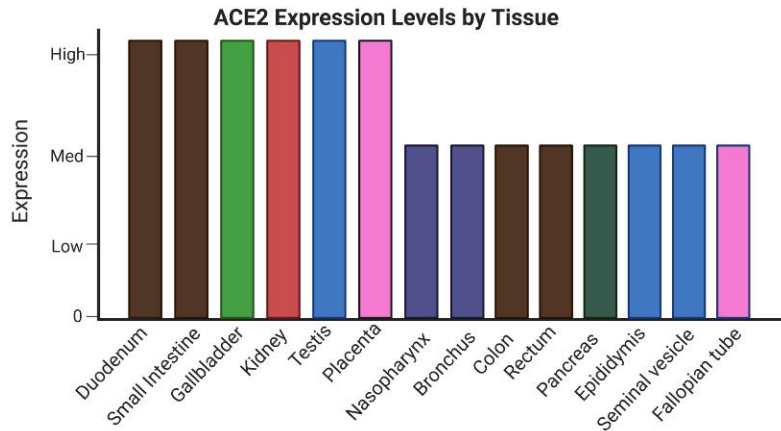
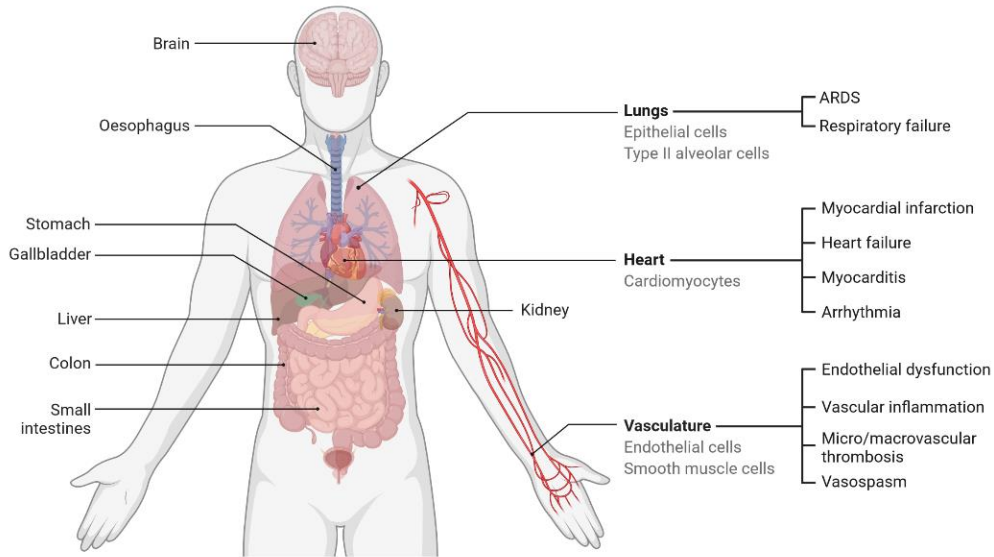


Figure 3. ACE2 tissue expression. Visual recreation of data gathered by The Human Protein Atlas project for tissue ACE2 expression that can be seen here <https://www.proteinatlas.org/ENSG00000130234-ACE2/tissue>.<sup>3</sup>

While the viral replicative cycle can cause direct damage to the host, most of the severe outcomes that have been observed in COVID-19 patients are due to the host's own immune response and the development of what has been termed the cytokine

<sup>3</sup> Figure Created with BioRender.com

storm, or cytokine shock syndrome<sup>20, 42, 48</sup>. This syndrome is characterized by a drastic increase in pro-inflammatory molecules that promotes widespread cell death.

With the recent advent of the novel mRNA COVID-19 vaccines from Pfizer and Moderna, the end of this deadly pandemic is in sight<sup>3, 38</sup>. However, until those vaccines can reach enough people to achieve herd immunity, coupled with the difficulties of mRNA vaccine dispersal and the rise of anti-vaccination sentiments among the populace, maintaining quick and accurate testing of COVID-19 infections is of paramount importance<sup>10, 53</sup>.

#### Current methods for testing of infectious diseases

The two most prevalent methods for diagnostic testing of infectious diseases are PCR and enzyme-linked immunosorbent assays (ELISAs). An overview of these two methods can be visualized in Figure 4. The major differences between the two methods are sample type used, ease of use, and the timepoints at which they can determine infection. PCR primarily uses a swab from the infectious site to check for genetic material, while ELISAs require a blood sample to be taken to ultimately utilize the serum to check for the presence of antibodies or antigens. PCR assays can be technically difficult, require a more fastidious process than ELISAs and must often undergo multiple steps on different instruments. In the clinical lab setting, ELISAs are a simple method to



utilize. After blood samples are collected, they are centrifuged and placed on an automated chemistry analyzer and the test can be completely automated.

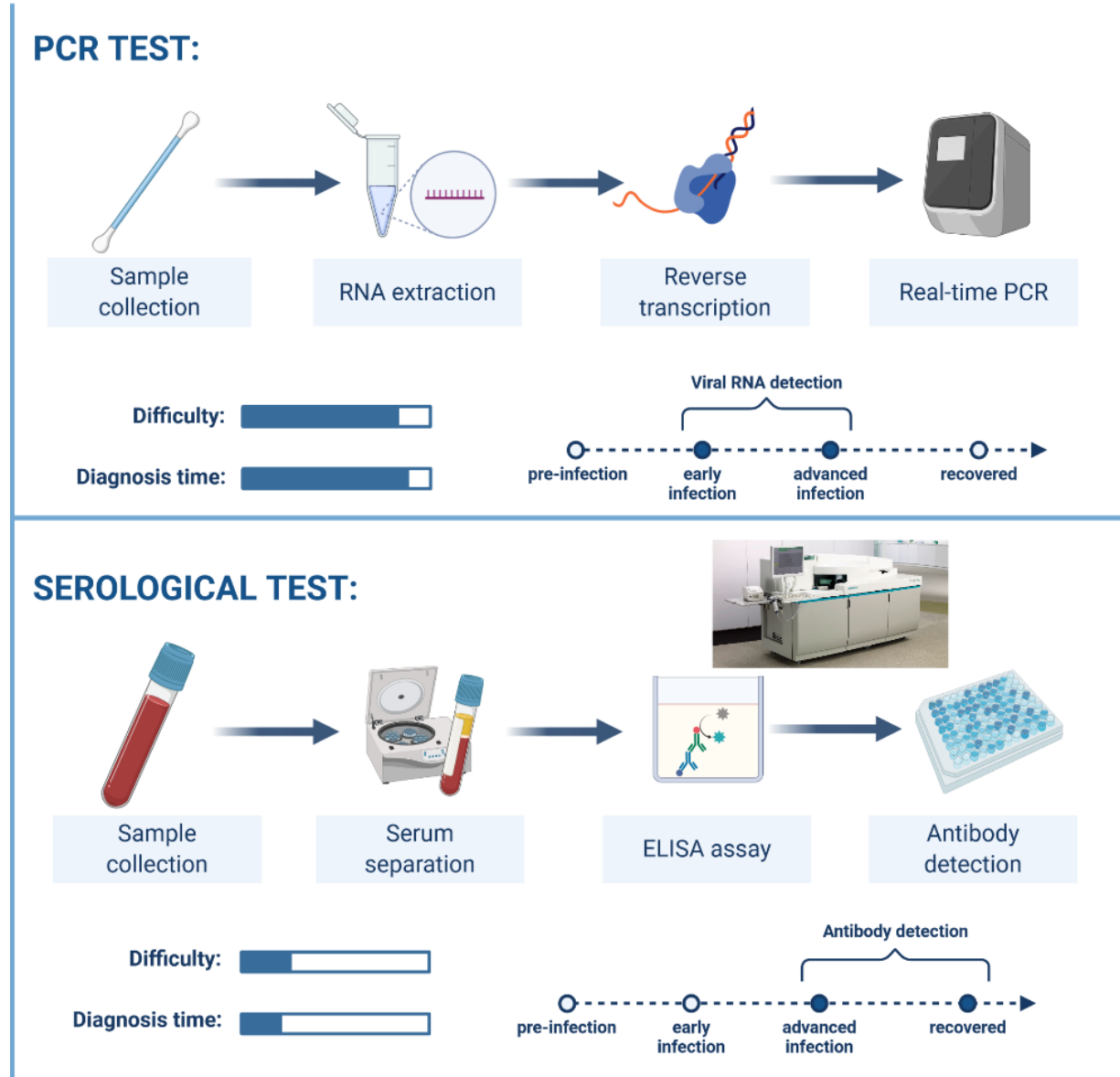


Figure 4. Infectious disease testing methods. A comparison between PCR testing and serological testing methods. <sup>4</sup>

<sup>4</sup> Figure Created with BioRender.com

While ELISAs sound like a better assay based on ease of use and reduced chance of user error because of automation, they have a severe drawback, the timepoints at which they can detect infection. PCR tests can determine if a patient is infected even at early stages, potentially before they begin showing symptoms but are already infectious. Patients will continue to test positive only while they have an active infection. This allows for accurate testing of active infections, which helps for monitoring disease spread and with the implementation of quarantine procedures. ELISAs on the other hand can only determine the presence of infection at later stages (once the immune system has responded and begun to produce antibodies). Patient samples will continue to test positive after an infection has resolved and the patient may no longer be actively infected or a source of spread. Based on these premises, PCR testing is usually the gold standard for infectious disease testing, especially in the case of epidemics and pandemics. It is for these reasons that the method utilized in this thesis and the method chosen by the CDC for COVID-19 testing is a PCR based assay. An overview of the CDC COVID-19 PCR test, with its specific primers and probes can be seen in Figure 5.

## COVID-19 Diagnostic Test through RT-PCR

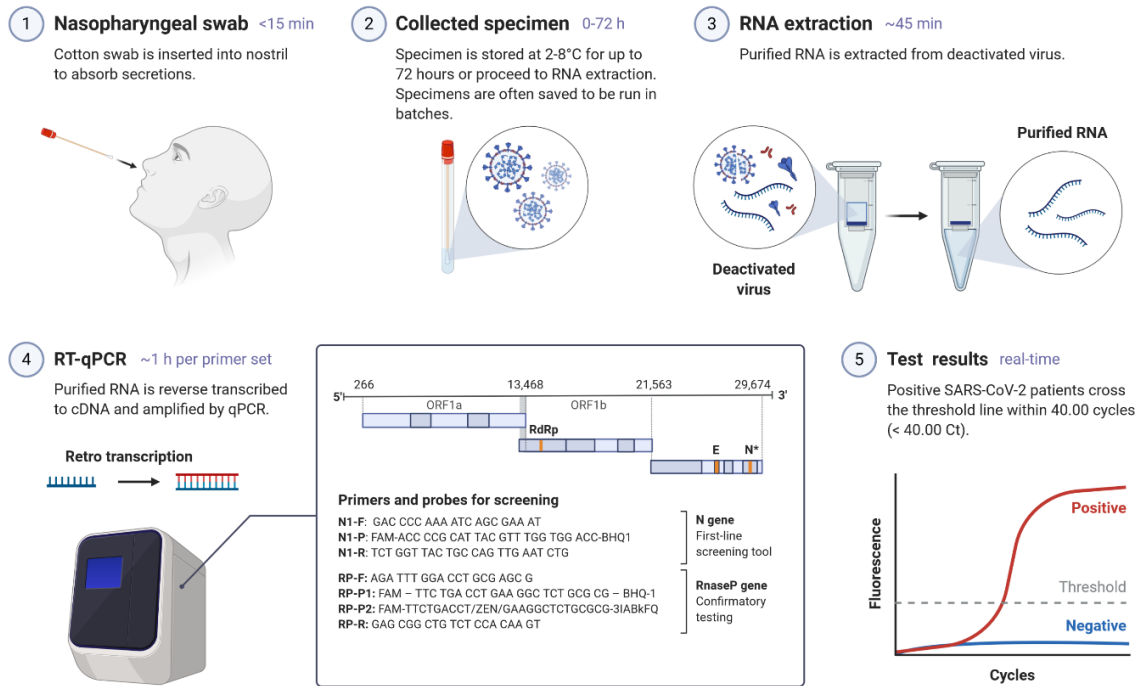


Figure 5. CDC COVID-19 N1-RnaseP probe-based qRT-PCR assay. <sup>5</sup>

## Polymerase Chain Reaction (PCR)

Polymerase Chain Reaction (PCR) was a method first developed in 1983 by Dr. Kary Mullis, and had its first published use in 1985<sup>25, 44</sup>. In his own words, it is a method that “lets you pick the piece of DNA you’re interested in and have as much of it as you want”<sup>34</sup>. PCR requires a reaction mixture of dNTPs, salts, primers, a DNA template, and a thermostable DNA polymerase. It can be broken down into three basic steps: (1) denaturation, where double stranded DNA (dsDNA) is heated until it unzips into single stranded DNA (ssDNA); (2) annealing, where the temperature is lowered to

<sup>5</sup> Figure Created with BioRender.com

allow for primers (short flanking DNA molecules) to bind; (3) extension, when DNA polymerase extends the 3' end of each primer along the template strand. These three steps are then repeated to exponentially increase the DNA targeted by the primers (Figure 6).

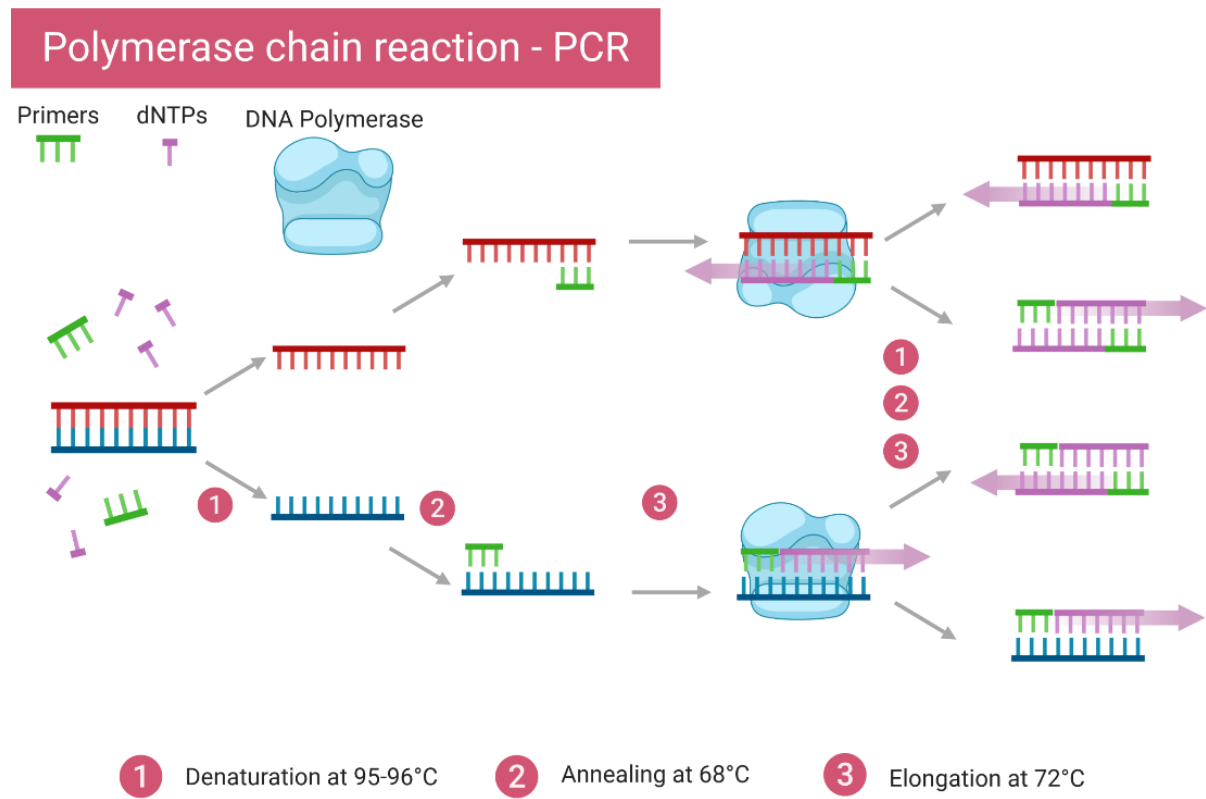


Figure 6. Polymerase Chain Reaction - PCR basic steps. <sup>6</sup>

The intricacies that come with developing an effective PCR assay revolve around the reaction mixture components and the cycling conditions. The DNA template, primer

<sup>6</sup> Figure Created with BioRender.com

design, sample source, and many other factors all play a role in assay design. Different DNA templates have different melting points based on length, GC content, and salt concentration. An increase in any of those parameters will cause an increase in the melting point (increased denaturation temperature), requiring a polymerase that can handle this increase in temperature<sup>12, 47, 52</sup>. An increase in GC content causes an increase in the number of relative hydrogen bonds for a given length of DNA as GC bonds contain three hydrogen bonds versus the two of AT bonds<sup>47, 52</sup>. Increasing the salt concentration shields the antiparallel strands from the negative charge of their phosphate groups, allowing for easier formation of hydrogen bonds<sup>47, 52</sup>. Parameters can be further affected based on primer concentration, primer delivery method, and polymerase type and concentration. An example formula for calculating the melting temperature of a double stranded oligonucleotide is:

$$T_m = \frac{\Delta H \times 1000}{\Delta S + (\text{Salt Correction}) + 1.9872 \ln \left( [A] - \frac{[B]}{2} \right)}$$

The common salt correction used is:

$$(0.368)(N - 1) \ln([mono^+] + 3.795\sqrt{[free Mg^{++}]})^{45}.$$

$\Delta H$  and  $\Delta S$  are the enthalpy and entropy, respectively, of base stacking adjusted helix initiation factors, [A] and [B] are the concentration of each strand of DNA, and  $[mono^+]$  is the concentration of monovalent cations<sup>45</sup>.

### Polymerase Improvements

The first iteration of PCR was rather inefficient due to the use of the Klenow fragment which was thermolabile and required new additions after every thermal cycle<sup>25</sup>,

<sup>33, 34</sup>. The Klenow fragment is a large protein subunit that is produced by treatment of DNA polymerase I from *E. coli* with the protease subtilisin <sup>13, 24</sup>. The Klenow fragment retains the 3' to 5' exonuclease and the 5' to 3' DNA polymerase domains and activity but loses the 5' to 3' exonuclease activity<sup>13, 24</sup>. The efficient and world changing method that we know today was not fully realized until the addition of a thermostable polymerase. Therefore, some may say that the story of PCR arguably begins with the discovery and isolation of *Taq* polymerase (a thermostable DNA polymerase isolated from *Thermus aquaticus*) in 1976<sup>6</sup>. *Taq* polymerase allowed for the uninterrupted thermal cycling conditions crucial to PCR, and, in 1988, when method met materials, PCR became a practical and revolutionary technique<sup>43</sup>. PCR was further improved upon by the development of a truncated *Taq* polymerase, called Klentaq, that lacks the 5' to 3' exonuclease activity, similar to the Klenow fragment and hence the similar naming, in 1993<sup>27</sup>. The full length *Taq* polymerase was still labile at temperatures above 90 degrees Celsius; however, the truncated form was able to withstand higher temperatures, allowing for longer DNA templates/products and DNA templates with higher GC contents to be utilized<sup>11, 25, 27</sup>. The increased thermal stability seen in Klentaq compared to the Klenow fragment is due to its reduced entropic penalty of folding<sup>28</sup>. Polymerases have been further improved upon by site directed mutagenesis and other experimental methods to increase stability, fidelity, efficiency and to tailor polymerases for specific uses<sup>2, 4, 11</sup>. The performance of these polymerases can be compared using Michaelis-Menten-like enzyme kinetics, where  $v = \frac{v_{max} [S]}{[S] + K_m}$  and  $K_m = (k_{off} + k_{cat}) / k_{on}$ <sup>26, 40</sup>.

The evolution of PCR (Hot start PCR, RT-PCR, qRT-PCR, extreme PCR)

Improvements to PCR have occurred through reaction mixture modifications as well as altering and improving upon the method itself. Some of the improvements and modifications to methodology include Hot start PCR, RT-PCR, qRT-PCR, and extreme PCR. Hot start PCR utilizes antibodies or aptamers that bind to the polymerase and will inhibit its activation until the temperature is raised during the thermal cycling<sup>21</sup>. This allows one to control the precise starting point of the polymerization and inhibits any potential early and erroneous amplification that may occur at ambient temperature<sup>21</sup>. RT-PCR, or reverse-transcription PCR, utilizes a reverse transcriptase (RT), an RNA-dependent DNA-polymerase, to reverse transcribe transcribe RNA to DNA. This allows for the detection and amplification of RNA viruses and is also utilized for gene expression analyses. RT-PCR requires an additional reverse transcription step prior to the normal cycling conditions. This reverse transcription step allows the RT to reverse transcribe the RNA present to DNA before the normal PCR steps can continue. qRT-PCR (quantitative real-time PCR) allows for “real-time” monitoring of the PCR process, speeds up testing results rapidly, and has become the gold standard for measuring cDNA and gDNA levels<sup>49</sup>. This real-time monitoring is achieved by the addition of fluorophores that emit a wavelength of light that a detector can sense as the PCR instrument is running. If there is no amplification, then no light is emitted by the fluorophores. There are two methods for fluorophore addition that can be utilized in qRT-PCR. One is the use of an intercalating dye, that will only emit light once it intercalates into double stranded DNA. Thus, as the amount of double stranded DNA increases through PCR, the amount of light produced increase. While extremely useful,

this method has a significant drawback in a lack of sensing specificity. Any DNA that is amplified, whether the intended target or not, will cause an increase in fluorescence. A more specific method is to utilize a probe-based assay where the probe has a fluorophore and quencher integrated into the probe itself. This method allows for only light to be emitted when there is amplification of the intended target and is the method utilized both by the CDC COVID-19 detection assay, and the method developed in this thesis. Figure 7 gives a visual representation of how the fluorescent probe-based qRT-PCR assay works.

### Fluorescent Probe-Based Real Time PCR (qPCR)

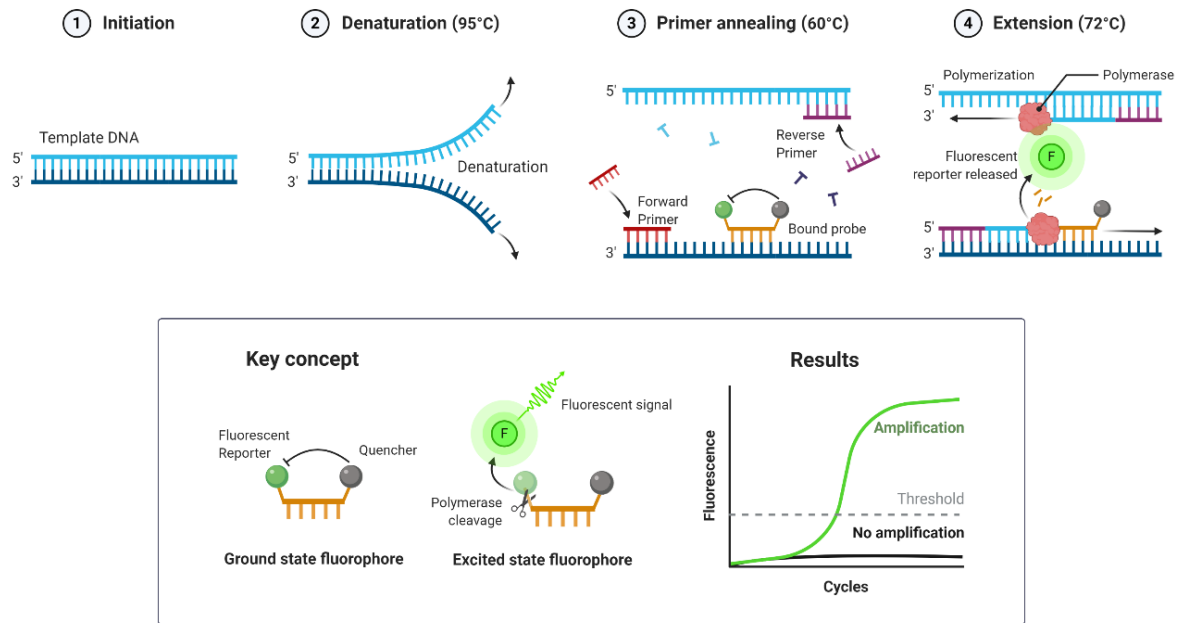


Figure 7. Fluorescent Probe-based Real Time PCR (qRT-PCR).<sup>7</sup>

<sup>7</sup> Figure Created with BioRender.com



Extreme PCR is a method recently developed at the University of Utah that drastically increases the speed at which PCR can occur, reducing completion time from hours to minutes or even seconds<sup>12, 32, 35</sup>, and with extreme one-step RT-PCR occurring in as little as 2 minutes<sup>39</sup>. PCR time to completion is inversely related to the reaction mixture components concentration, and by increasing those concentrations one can significantly reduce the time PCR takes<sup>12</sup>. Specifically, by increasing the polymerase and primer concentrations at roughly equal proportions such that there is enough polymerase to utilize all of the primers and enough primers for each polymerase to utilize. This increase in concentration can occur by reducing the reaction volume and/or by increasing the amount of reaction components used. The other key factor in the speed of extreme PCR is its ability to rapidly cycle the temperature conditions. The difference in thermal cycling conditions between Extreme PCR and Conventional PCR can be observed in Figure 8.

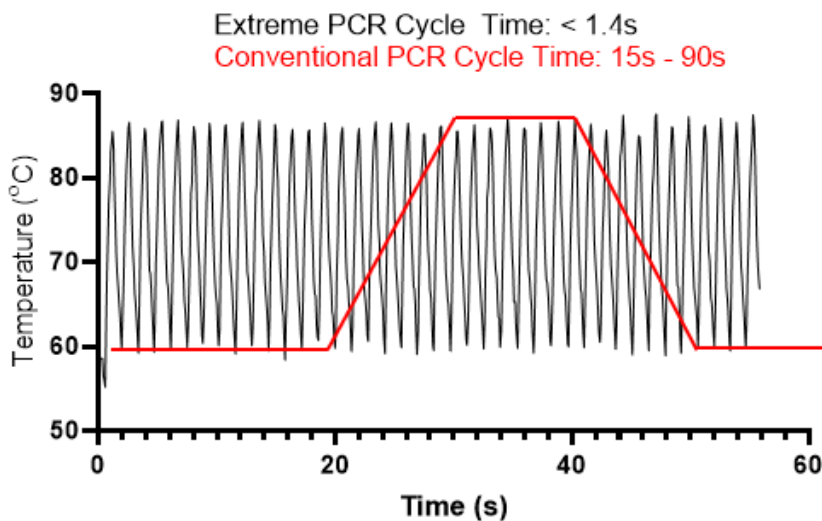


Figure 8. Extreme PCR vs Conventional PCR

In extreme PCR, samples are placed in glass capillary tubes (the thermal conductivity of glass is 5 to 10 times greater than that of plastic at a given thickness, allowing for more rapid thermal cycling conditions) that are rapidly oscillated between a hot and cold-water bath by a stepper motor.

This thesis will explore improvements to current SARS-CoV-2 testing methodologies to improve patient sampling to result times. Consequently, providing possible improvements to patient clinical outcomes as well as improvements to quarantining procedures. This thesis looks at both extraction-free methodologies, skipping the nucleic acid extraction step (step 3 in figures 5 and 9), in a rapid PCR assay using clinical grade equipment to provide the basis of a ready to implement clinical assay for SARS-CoV-2 testing as well as an extraction-based method using extreme PCR to elucidate the time gating bottlenecks in current PCR testing procedures.

## Materials and Methods

### Specimen acquirement and storage

Nasopharyngeal swabs were collected in 1mL of universal transport media (UTM; BD). For spiked samples, the indicated amounts of SARS-CoV-2 inactivated virus were added to universal UTM and were subsequently processed. Briefly, samples were mixed in a 2:1 ratio of sample and 20% Triton-X100, then vigorously vortexed for 3

pulses of 5 seconds each. Following vortexing, samples were centrifuged at 20,000g for 15 seconds to pellet cell debris. 3.0 µL of supernatant was then used for each reaction.

Positive patient samples were kindly provided by the University of Washington clinical virology laboratory. Briefly, samples were provided on dry ice in UTM or viral transport media (VTM). All samples had previously tested positive using either the University of Washington SARS-CoV-2 Real-time RT-PCR assay or Panther Aptima TMA for SARS-CoV-2. Quantification value (Cq) for the University of Washington SARS-CoV-2 Real-time RT-PCR assay and relative luminescence units (RLU) values for the Panther Aptima TMA were also provided.

#### Primers

The SARS-CoV-2 N1 CDC primer and probes were used for LightCycler-based assays, as seen in Figure 5. Primers targeting the N gene were chosen because it is vital for viral replication and is not under selective immune pressure, as say the spike protein, aiding to its conserved nature. Primers for extreme PCR require higher annealing temperatures than traditional PCR primers and were designed using the NCBI PrimerBlast. Adjusted NCBI PrimerBlast parameters were: optimal annealing temperatures were set to 67°C, oligonucleotide concentration to 10,000 nmol/L, optimal product melting temperature to 80°C. Primers were then blasted against all virus, bacteria and human Reference Sequences using NCBI PrimerBlast to ensure there would be no off-target amplification. Primer sequences can be found in Table 1.

Table 1. SARS-CoV-2 primers

Name	Sequence (5' → 3')
CDC_N1_F	GACCCCAAATCAGCGAAAT
CDC_N1_R	TCTGGTACTGCCAGTTGAATCTG
CDC_N1_probe	FAM-ACCCCGCATTACGTTTGGTGGACC-BHQ1
Extreme_N2_F	CATTGGCATGGAAGTCACACCT
Extreme_N2_R	CCAATTTGATGGCACCTGTGTA

#### Reagents

SARS-CoV-2 viral RNA, SARS-CoV-2 inactivated virus, and SARS-CoV-2 quantitative synthetic RNA were acquired from BEI Resources and used for spiking samples and as positive controls.

#### Mastermixes

For extreme RT-PCR, we performed reactions in 5 $\mu$ L volumes containing 50 mmol/L Tris (pH, 8.3), 3 mmol/L MgCl<sub>2</sub>, 200  $\mu$ mol/L of each dNTP (dATP, dCTP, dGTP, dTTP), 500  $\mu$ g/mL nonacetylated BSA (Sigma), 2% (vol/vol) glycerol (Sigma), 10.0  $\mu$ mol/L of each primer, 1U/ $\mu$ L KlenTaq1, 2X LunaScript RT Enzyme Mix (NEB), and 2.5  $\mu$ mol/L Syto9 (Life Technologies). Due to the high concentrations of polymerase and primers, reactions were prepared on ice to avoid non-specific amplification and primer-dimer formation.

For rapid PCR conducted on the capillary-based LightCycler 1.5 (Roche), Luna Probe One-Step RT-qRT-PCR 4x Mix with UDG (NEB) was used. Reactions were performed in 10 $\mu$ L volumes containing 5  $\mu$ mol/L of each forward and reverse primers for indicated targets and 250nmol/L of probe for each indicated target.

#### Melt curve analysis

HR-1 from Idaho Technologies was used to generate melt curves. For experiments comparing relative productive amounts, LED voltages were kept constant when comparing relative product amounts. The data were analyzed with custom-created software written in LabView and viewed as the derivative of the melting curves<sup>37</sup>.

#### PCR Thermocycling conditions

For LightCycler-based assays the parameters used were: RT was set to 55°C for the indicated times, annealing/elongation temperatures were set to 63°C, the melt/denaturation step was set to 95°C for a 0s hold, and ramp rates were 20°C/s for all experiments. The schematic for our extraction-free method can be seen in Figure 9.

## SARS-CoV-2 testing procedure schematic

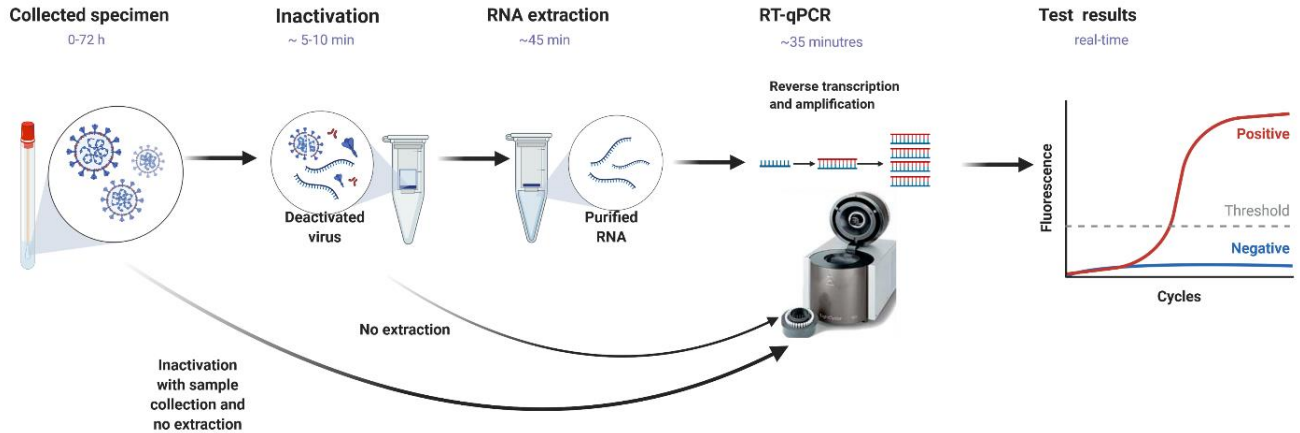


Figure 9. SARS-CoV-2 testing procedure schematic. <sup>8</sup>

The setup for extreme PCR can be visualized in Figure 10. For extreme PCR, a hot bath at 100°C and a cool water bath at 60°C were used for thermal cycling parameters. The water baths were heated on electric hotplates with temperature monitoring using an Omega OMB-DAQ-56 USB data acquisition module and Type-T thermocouples (Omega 5SRTC-TT-T-40-36). A stepper motor (stepper online, model #23HS41-1804S), driven by a digital stepper drive (stepper online, DM542T) with pulse and direction signaling provided by an Arduino Uno R3 (Sparkfun) rotated samples in a custom sample holder between each water bath in <math><0.2\text{s}</math>. The stepper motor was controlled using a custom LabView program similar to software previously described<sup>12</sup>. A thermocouple (Omega type T precision fine wire thermocouple, 0.003-inch diameter with Teflon insulation) centered in a dedicated control tube was used to measure

<sup>8</sup> Figure Created with BioRender.com

temperature and trigger stepper motion. Stepper motor motion was triggered at 84°C for denaturation and 67°C for annealing/extension to obtain desired temperature cycling profiles for 40 cycles. RT was performed for the indicated amount of time in the cool bath at 60°C for indicated times immediately prior to thermocycling. All reactions were conducted in standard Roche LightCycler capillaries.

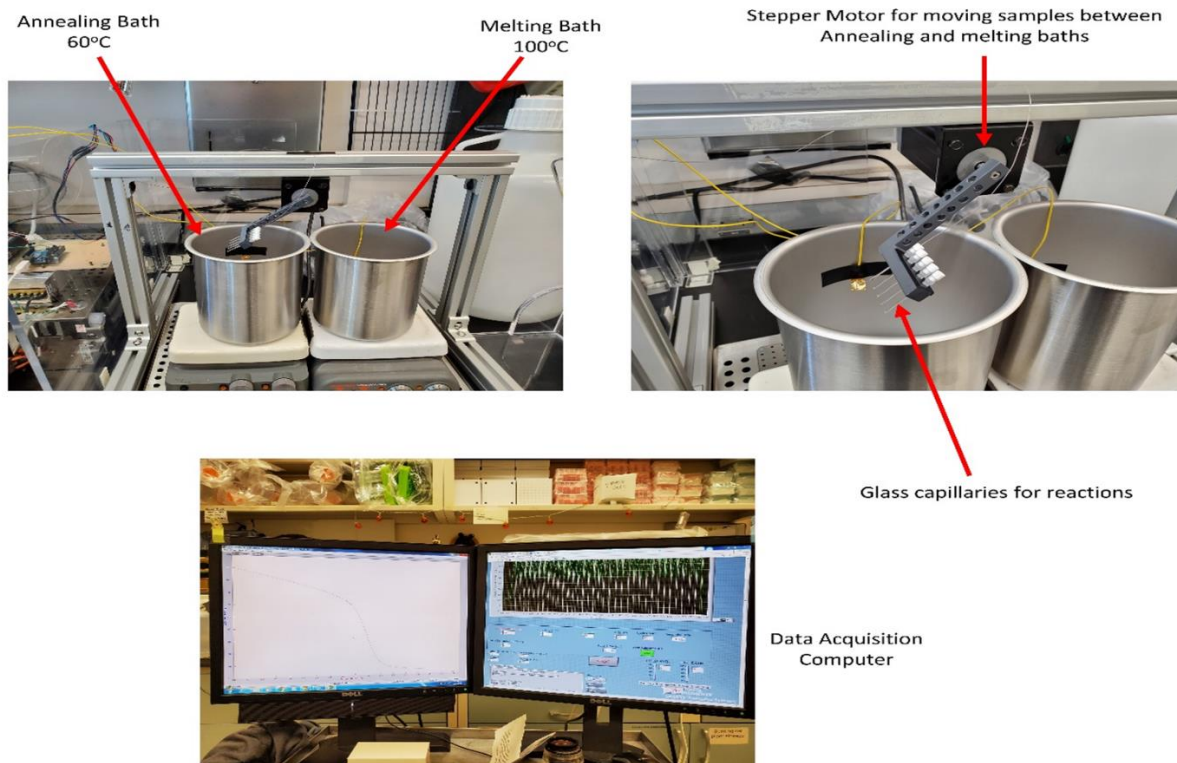


Figure 10. Extreme PCR setup

### RT optimization

10  $\mu$ L reactions were prepared on ice. Samples were incubated in a 55°C water bath for indicated amounts of times followed by a 5-minute incubation in boiling water for reverse transcriptase inactivation. Samples were quickly placed on ice until

thermocycling. Samples were thermocycled as above with a 10s annealing/extension step. For the 0s RT timepoint, samples were added to boiling water without any incubation at 55°C.

#### PCR cycle time optimization

10 µL reactions were prepared on ice. RT was conducted in a 55°C water bath for 10 minutes followed by a 5-minute incubation in boiling water for reverse transcriptase inactivation. Samples were quickly placed on ice until thermocycling. Samples were thermocycled for indicated times. For the 0s timepoint, the hold time for annealing/extension at 63°C was set to 0s.

## Results

#### RT optimization

While it has been shown that reverse transcription can be conducted faster than manufacturer's recommend, we wanted to determine the shortest amount of time required for efficient RT<sup>39</sup>. Typical primer concentrations for extreme RT-PCR range from 5-20 µmol/L<sup>12, 39</sup>. Because of our reduced polymerase concentrations, and slower thermocycling conditions, as compared to extreme RT-PCR, we would be unable to efficiently use the higher concentration levels; therefore, we used 5 µmol/L primer concentrations. We chose to utilize the Luna Warm Start Reverse Transcriptase



because of its aptamer based warm start inhibition, the reversibility of this warm start formulation, as well as its increased thermostability. We utilized the CDC N1 SARS-CoV-2 primer set for a proof of principle.

Previous studies examining rapid RT primarily utilized isolated RNA<sup>39</sup>. As we also wanted to optimize this assay for extraction free testing, we examined the time requirements for RT with pure RNA, RNA spiked into diluent from a NP swab from an uninfected control as well as 10 samples for which the patients had tested positive (prepared as in methods). After setting up reactions on ice, we incubated the reaction tubes at 55°C for indicated amounts of time. Following indicated incubation times, we quickly transferred the reaction capillaries to a boiling water bath (100°C) for 5 minutes to denature the reverse transcriptase and subsequently transferred the tube to an ice water bath. Reactions were then subjected to PCR amplification using a LightCycler 1.5 with 30s annealing/extension times.

We saw efficient RT within 30s for both pure RNA as well as RNA spiked into an uninfected control (Figs. 11A-C). However, we saw variation between extraction-free positive patient samples for the optimal time required for RT (Fig. 11D), on average requiring >5 minutes for efficient RT (Figs. 11E-F). Only a small decrease in cycle counts were observed with increasing RT concentrations as previously predicted due to our lower polymerase concentrations and slower thermocycling conditions (Fig. 11F-G), and a negligible difference in cycle count between the 4x and 2x RT concentrations past 10 seconds (Fig. 11F-G).

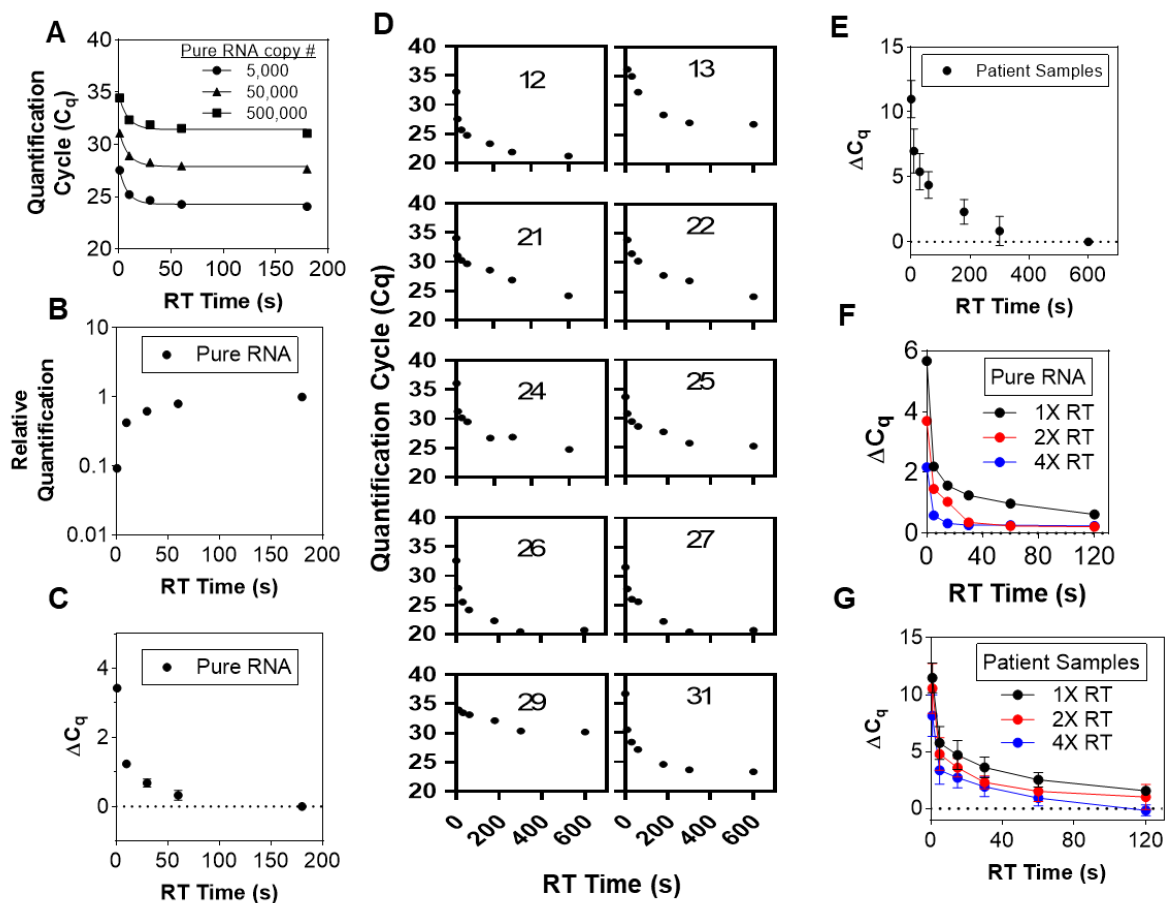


Figure 11. **Reverse Transcription Optimization:** (A) Varied concentrations of SARS-CoV-2 genomic RNA were spiked into water or an uninfected control NP swab diluent and RT was conducted for indicated amounts of time followed by PCR. (B) Relative quantification based on the ddCq relative to the longest RT time point. (C) Difference in Cq values between the longest time point and indicated time points for spiked samples. (D) Positive patient samples had RT conducted for indicated time amounts followed by PCR, numbers in each figure corresponds to the patient sample used. (E) Difference in Cq values between each time point based on the ddCq relative to the longest RT time point. (F) SARS-CoV-2 genomic RNA was spiked into UTM media and ran with 1X, 2X, or 4X RT, and reverse transcription was performed for the indicated times. (G) Positive SARS-CoV-2 patient samples were ran with the amount of RT indicated and reverse transcription was performed for the indicated times.

### PCR cycle optimization

Because previous studies have reported inhibition when using extraction-free samples for SARS-CoV-2 RT-PCR, determining an optimal PCR protocol for our methods was crucial. Most commercial RT-PCR assays for SARS-CoV-2 have an

annealing/extension time of  $\geq 30$ s per cycle and we wanted to determine the efficacy of reduced cycle times. Previous studies show that annealing/extension times of  $< 0.5$ s per cycle can be performed; however, those studies were performed on purified DNA. To determine the efficacy of both methods of detection for qRT-PCR, our study utilized probe-based detection for our light cycler method and used intercalating dyes for our Extreme PCR method. Purified RNA, or extraction-free positive patient samples, were used to test for the optimal time required for our assay. Samples were all reverse transcribed for 10 minutes prior to thermocycling.

A difference of only 1 cycle count was observed for purified RNA when comparing a 0s vs 30s annealing/extension step. This suggests that efficient PCR in our assay can be done rapidly and far faster than common commercially available RT-PCR assays for SARS-CoV-2 (Figs. 12A, C, D). However, extraction-free positive patient samples required a 10s annealing/elongation step for efficient PCR (Fig. 12B), which still significantly reduces the time it takes for patient sample processing compared to the current common annealing and extension time of  $\geq 30$  seconds. Cumulatively, we saw almost no difference in Cq values between samples with 10s vs. 30s annealing/elongation (Figs. 12C-D).

Using a 10s annealing/elongation step, we next examined the efficiency of our reaction using pure RNA as well as RNA spiked into diluent from a NP of an uninfected control. Both the pure RNA and spiked NP sample were efficient with efficiencies of 100.3% and 109.9%, respectively (Figs. 12E-F). Additionally, 20/20 reactions with 3 copies/reaction tested positive in the spiked NP sample suggesting an LOD of 1.5 copies/mL (Fig. 12G). We then determined the effects of increasing polymerase and

primer concentrations on Cq of patient samples. A decrease to cycle count was only observed when increasing the primer concentration to 5 $\mu$ M from 1 $\mu$ M, and no significant change between 5 $\mu$ M, 10 $\mu$ M, and 15 $\mu$ M primer concentrations (Fig. 12E). For polymerase concentration testing we only saw an approximately 1 to 1.5 cycle count change, depending on the patient sample, when increasing the polymerase concentration from 1X to 5X (Fig. 12D). This difference is ultimately negligible and not beneficial when considering the increased cost per sample. No significant change in cycle count was observed between the 5X and 10X concentrations (Fig. 12D). Based on these results, we concluded that utilizing 5 $\mu$ M primer concentrations (anything greater would place us within the extreme PCR patent held by Witter, Farrar, and the University of Utah WO2013177429A2), and 1X polymerase concentrations were ideal for our protocol when considering speed, efficiency, specificity, and cost.

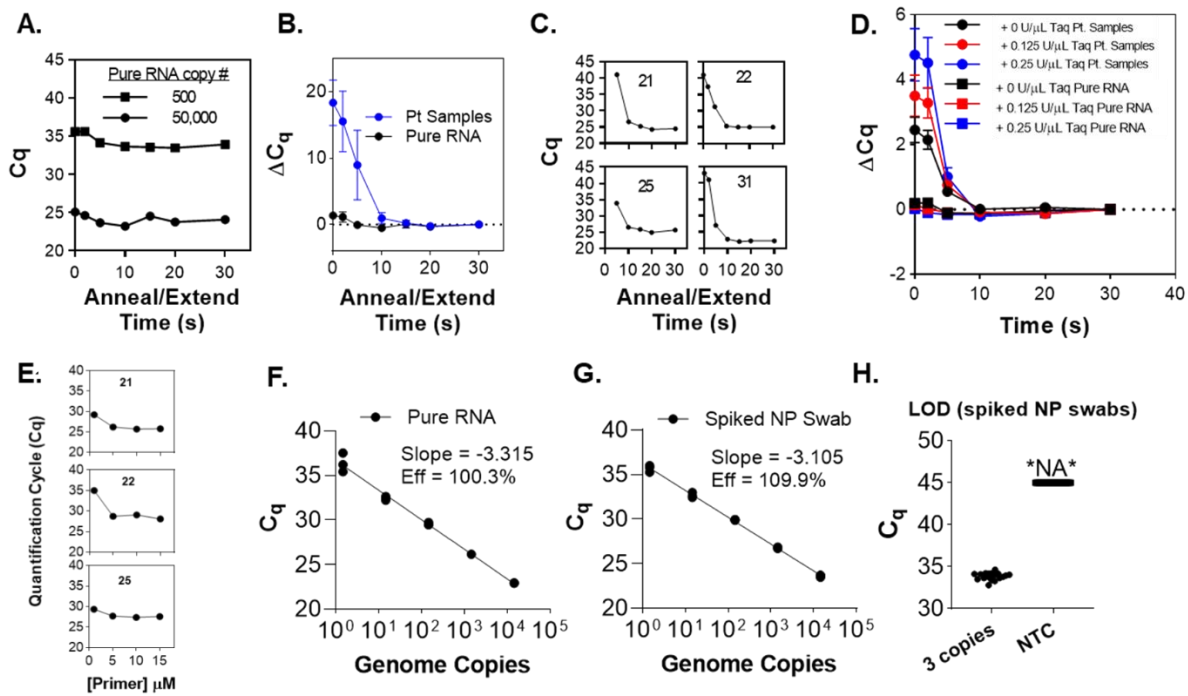
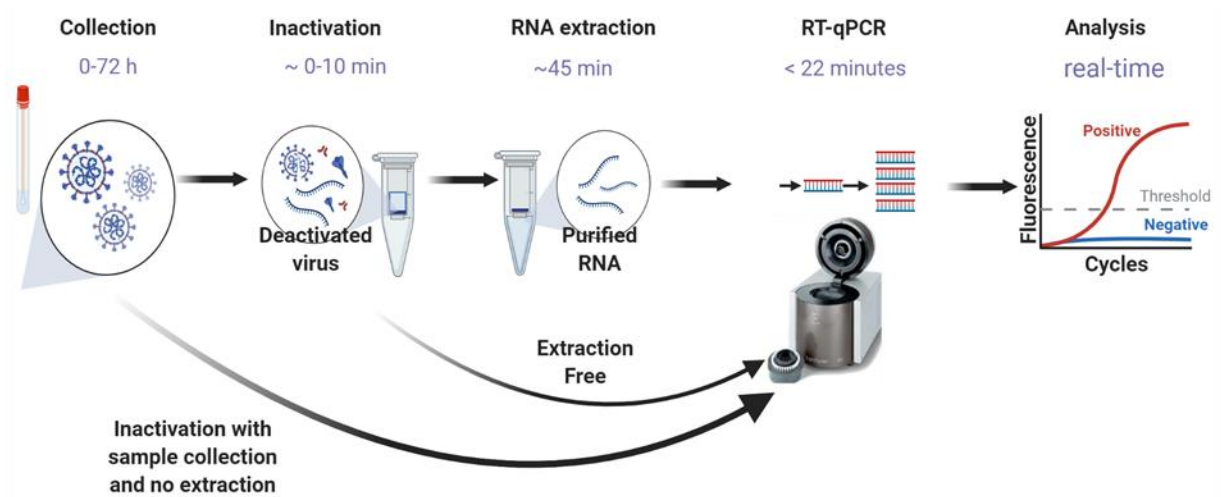


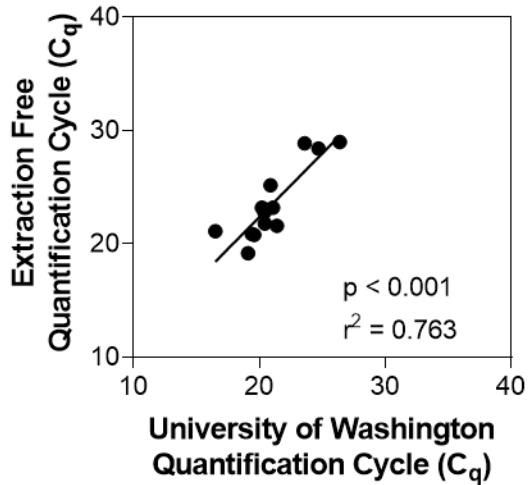
Figure 122. **PCR cycle time optimization:** (A) Two concentrations of SARS-CoV-2 genomic RNA were spiked into water and RT was conducted for 10 minutes followed by PCR with varied annealing/elongation cycle times. (B) Difference in Ct values between the longest cycle time and indicated annealing/extension times. (C) Positive patient samples were reverse transcribed for 10 minutes followed by PCR for varied annealing/elongation cycle times. (D) 0 U/ $\mu$ L, 0.125 U/ $\mu$ L, and 0.25 U/ $\mu$ L of Taq polymerase were added to the samples shown above for the indicated annealing/extension times. (E) Patient samples shown were ran with the primer concentrations shown. (F) Efficiency of dirLC assay using SARS-CoV-2 genomic RNA spiked into water. (G) Efficiency of dirLC assay using SARS-CoV-2 genomic RNA spiked into uninfected control NP swab diluent. (H) LOD assay for dirLC using SARS-CoV-2 genomic RNA spiked into uninfected control NP swab diluent.

## Direct Light Cycler Validation

Based on our optimization studies, we adopted an RT-PCR protocol which consisted of a 5-minute RT step at 55°C followed by a 10s denaturation step at 95°C. This was then followed by 45 cycles of PCR with a 10s annealing/elongation at 63°C with a 0s hold time at 95°C, allowing our protocol to have results in under 30 minutes. 41 positive patient samples, obtained from the University of Washington, were tested using this extraction-free testing protocol. Of the 41 University of Washington positive patient samples, 16 of the 42 samples were originally run on the University of Washington SARS-CoV-2 Real-time RT-PCR assay, and the remaining 26 were run on Panther Aptima TMA. 40/41 samples tested positive on our platform. For the 15/16 samples in which we had Cq values from the original testing, a correlation analysis was performed and saw a significant correlation,  $R^2 = 0.763$  (Fig. 13). No correlation between our Cq values and RFU from the 26 samples originally run on the Panther Aptima TMA platform was observed (Fig. 13). This was an expected result as the Panther Aptima TMA platform is an endpoint qualitative assay versus the real-time quantitative assay of our light cycler protocol. For the one sample which did not test positive with our protocol, the original Cq values on the University of Washington SARS-CoV-2 Real-time RT-PCR assay platform were 37.1 for one replicate and not detected for the other replicate.



**B.**



**C.**

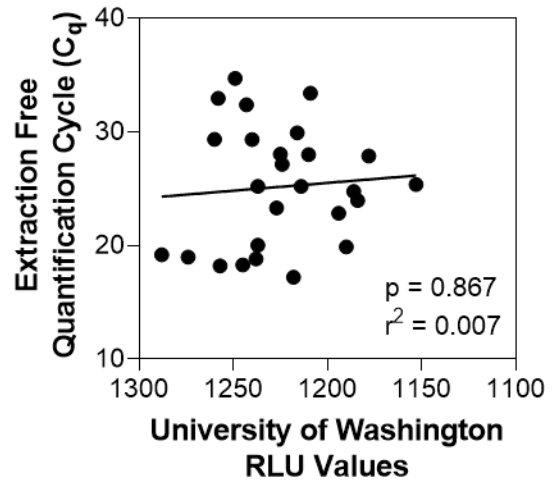


Figure 13. **Direct Light Cycler validation:** (A) Schematic diagram of the direct LightCycler protocol. (B) Correlation analysis between Ct values from dirLC and Ct values obtained originally during testing at the University of Washington Clinical Virology Laboratory. (C) Correlation analysis between Ct values from dirLC and RLU values from the Panther Aptima TMA assay conducted on the original samples at the University of Washington Clinical Virology Laboratory.

## Extreme RT-PCR for SARS-CoV-2

While our protocol on the LightCycler allowed for successful detection of SARS-Cov-2 in < 30 minutes using extraction-free methodologies and clinically available and pertinent equipment and reagents, we also wanted to examine and compare the overall time for testing using RNA extraction, followed by extreme RT-PCR (Fig. 14A). Because extreme RT-PCR utilizes different concentrations, cycling conditions, and is designed to amplify shorter products, we needed to design and use a different primer set targeting the nucleocapsid gene of SARS-CoV-2 (Table 1). Successful amplification of the desired target was measured by high resolution melt curve analysis of the product. Using a 30s RT step and ~1.2s PCR cycles, we were able to successfully amplify purified SARS-CoV-2 genomic RNA with successful amplification down to 4 copies/reaction (Fig. 14B). Additionally, we saw successful amplification of SARS-CoV-2 RNA spiked into NP swab diluent from a healthy, uninfected control (Fig. 14C). However, we did not see successful amplification of positive patient samples which is not surprising considering the results from Figures 1-2. Overall, the extreme RT-PCR followed by high resolution melting required < 3 minutes. This data suggests that even with the extreme speed of extreme RT-PCR the significant chokepoint on time is the genomic isolation step. For future assays, the fastest testing methodologies will be those that can utilize extraction-free methodologies or new technologies that improve upon extraction speed and use it in conjunction with extreme RT-PCR.



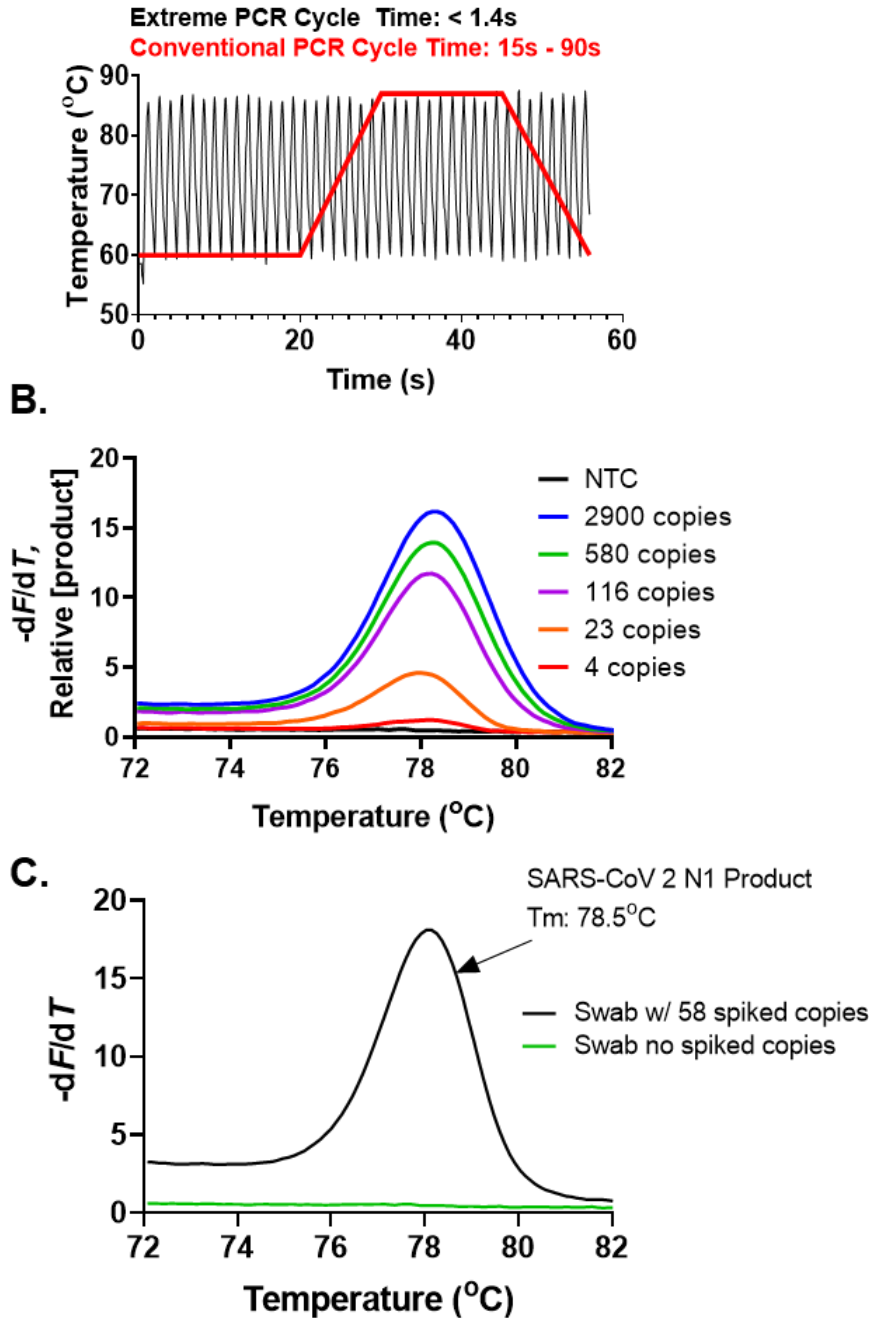


Figure 14. **Extreme RT-PCR for SARS-CoV-2:** (A) Representation of cycling time in extreme PCR (black) vs. traditional cycling times (red). (B) Melt curve analysis from extreme RT-PCR was conducted on SARS-CoV-2 genomic RNA spiked into water. The height of the melt peak is relative to final product concentration. (C) Melt curve analysis post-extreme RT-PCR was conducted on SARS-CoV-2 genomic RNA spiked into uninfected control NP swab diluent.

## Discussion

COVID-19, as of January 17<sup>th</sup>, 2021, currently ranks 9<sup>th</sup> on the death toll list for global pandemics, with over 2 million deaths and counting. The best way to mitigate spread and death prior to vaccination is with rapid, easy to use, and accurate testing. Not only does fast and accurate testing methodology for infectious disease help with the prevention of spread but also serves to improve clinical outcomes for infected patients. With the recent development and deployment of the Moderna and Pfizer mRNA COVID-19 vaccines<sup>3, 38</sup>, there is an end in sight to this devastating pandemic; however, until those vaccines are able to can be administered to enough people to reach a level of herd immunity, and with the rise of new variants which the vaccines may not confer protection against, fast and accurate testing remains of the utmost importance in preventing further spread. The testing outlined in this thesis is also unaffected by the rise of the new SARS-CoV-2 variants as the mutations that have occurred are all located in the spike protein due to immune selective pressure. The methods utilized in this thesis all target the conserved nucleocapsid gene because it is not under immune selective pressure and is likely to remain unchanged. Rapid and accurate testing for infectious diseases also allows for proper quarantining procedures, minimizing the time a patient must wait to determine if quarantining is necessary, and, determines when viral shedding has completed and if quarantining is no longer necessary. This aids in reducing patient and hospital costs and improves patient and healthcare worker overall health and safety.

Several novel testing methods have been developed during the COVID-19 pandemic that have had varying degrees of success or feasibility, but shortages and

delayed testing has continued to plague us during this pandemic and the necessity of fast and accurate testing has remained absolute<sup>1, 18, 19, 23, 30, 31, 46, 51</sup>. We sought to determine methods that would allow for faster and accurate testing methods that improve upon the currently available RT-PCR methodologies often take greater than 60 minutes per patient while remaining economically viable to testing facilities. By skipping the genomic isolation step, extraction-free methodologies save on both time and cost, with genomic isolation often taking approximately 45 minutes, making total sample to result time take hours.

Our studies show that extraction-free RT-PCR is a viable clinical diagnostic assay that can drastically reduce patient testing even when using patient samples shipped across country from the University of Washington. Some difference was observed between the spiked samples and actual patient samples, suggesting some potential inhibition either due to patient mucus or immune mediators; however, all samples still coincide with clinical assay results. This further confirms that optimization studies require the use of samples from infected patients rather than uninfected spiked samples. We show that extraction-free RT-PCR requires 5 to 10 minutes for efficient RT and 10s annealing/extension per cycle for 45 cycles gives accurate and sensitive results in under 30 minutes. Using isolated RNA, RT-PCR can be further shortened to an RT of <30s and <60s for PCR. The use of more robust polymerases that are resistant to the source of inhibition may further speed up the reaction time for extraction-free methodologies.

The methods developed in this research provides an insight into the increases in speed of PCR diagnostic assays that can be implemented and further built upon for

infectious disease testing now and in the future. The use of clinically approved instruments (Roche LightCycler) and commercially available RT-PCR reagents with the data obtained using the LightCycler protocol allow for immediate clinical translation and use.

## References

1. Abbasi, J. "Crispr-Based Covid-19 Smartphone Test in Development." *JAMA* 325, no. 6 (Feb 9 2021): 522. <https://doi.org/10.1001/jama.2021.0493>.  
<https://www.ncbi.nlm.nih.gov/pubmed/33560305>.
2. Aschenbrenner, J., S. Werner, V. Marchand, M. Adam, Y. Motorin, M. Helm, and A. Marx. "Engineering of a DNA Polymerase for Direct M(6) a Sequencing." *Angew Chem Int Ed Engl* 57, no. 2 (Jan 8 2018): 417-21.  
<https://doi.org/10.1002/anie.201710209>.  
<https://www.ncbi.nlm.nih.gov/pubmed/29115744>.
3. Baden, L. R., H. M. El Sahly, B. Essink, K. Kotloff, S. Frey, R. Novak, D. Diemert, et al. "Efficacy and Safety of the Mrna-1273 Sars-Cov-2 Vaccine." *N Engl J Med* (Dec 30 2020). <https://doi.org/10.1056/NEJMoa2035389>.  
<https://www.ncbi.nlm.nih.gov/pubmed/33378609>.
4. Blatter, N., A. Prokup, A. Deiters, and A. Marx. "Modulating the Pka of a Tyrosine in KlenTaq DNA Polymerase That Is Crucial for Abasic Site Bypass by in Vivo Incorporation of a Non-Canonical Amino Acid." *Chembiochem* 15, no. 12 (Aug 18 2014): 1735-7. <https://doi.org/10.1002/cbic.201400051>.  
<https://www.ncbi.nlm.nih.gov/pubmed/24764289>.
5. Braun, J., L. Loyal, M. Frensch, D. Wendisch, P. Georg, F. Kurth, S. Hippenstiel, et al. "Sars-Cov-2-Reactive T Cells in Healthy Donors and Patients with Covid-19." *Nature* 587, no. 7833 (Nov 2020): 270-74. <https://doi.org/10.1038/s41586-020-2598-9>.  
<https://www.ncbi.nlm.nih.gov/pubmed/32726801>.
6. Chien, A., D. B. Edgar, and J. M. Trela. "Deoxyribonucleic Acid Polymerase from the Extreme Thermophile Thermus Aquaticus." *J Bacteriol* 127, no. 3 (Sep 1976): 1550-7. <https://doi.org/10.1128/JB.127.3.1550-1557.1976>.  
<https://www.ncbi.nlm.nih.gov/pubmed/8432>.
7. Cui, J., F. Li, and Z. L. Shi. "Origin and Evolution of Pathogenic Coronaviruses." *Nat Rev Microbiol* 17, no. 3 (Mar 2019): 181-92. <https://doi.org/10.1038/s41579-018-0118-9>.  
<https://www.ncbi.nlm.nih.gov/pubmed/30531947>.
8. Daniloski, Z., T. X. Jordan, H. H. Wessels, D. A. Hoagland, S. Kasela, M. Legut, S. Maniatis, et al. "Identification of Required Host Factors for Sars-Cov-2 Infection in Human Cells." *Cell* 184, no. 1 (Jan 7 2021): 92-105 e16.  
<https://doi.org/10.1016/j.cell.2020.10.030>.  
<https://www.ncbi.nlm.nih.gov/pubmed/33147445>.
9. Dong, E., H. Du, and L. Gardner. "An Interactive Web-Based Dashboard to Track Covid-19 in Real Time." *Lancet Infect Dis* 20, no. 5 (May 2020): 533-34.  
[https://doi.org/10.1016/S1473-3099\(20\)30120-1](https://doi.org/10.1016/S1473-3099(20)30120-1).  
<https://www.ncbi.nlm.nih.gov/pubmed/32087114>.
10. Dror, A. A., N. Eisenbach, S. Taiber, N. G. Morozov, M. Mizrachi, A. Zigran, S. Srouji, and E. Sela. "Vaccine Hesitancy: The Next Challenge in the Fight against Covid-19." *Eur J Epidemiol* 35, no. 8 (Aug 2020): 775-79.  
<https://doi.org/10.1007/s10654-020-00671-y>.  
<https://www.ncbi.nlm.nih.gov/pubmed/32785815>.
11. Drum, M., R. Kranaster, C. Ewald, R. Blasczyk, and A. Marx. "Variants of a Thermus Aquaticus DNA Polymerase with Increased Selectivity for Applications in Allele-

- and Methylation-Specific Amplification." *PLoS One* 9, no. 5 (2014): e96640.  
<https://doi.org/10.1371/journal.pone.0096640>.  
<https://www.ncbi.nlm.nih.gov/pubmed/24800860>.
12. Farrar, J. S., and C. T. Wittwer. "Extreme Pcr: Efficient and Specific DNA Amplification in 15-60 Seconds." *Clin Chem* 61, no. 1 (Jan 2015): 145-53.  
<https://doi.org/10.1373/clinchem.2014.228304>.  
<https://www.ncbi.nlm.nih.gov/pubmed/25320377>.
  13. Green, M. R., and J. Sambrook. "E. Coli DNA Polymerase I and the Klenow Fragment." *Cold Spring Harb Protoc* 2020, no. 5 (May 1 2020): 100743.  
<https://doi.org/10.1101/pdb.top100743>.  
<https://www.ncbi.nlm.nih.gov/pubmed/32358055>.
  14. Hoffmann, M., H. Kleine-Weber, S. Schroeder, N. Kruger, T. Herrler, S. Erichsen, T. S. Schiergens, *et al.* "Sars-Cov-2 Cell Entry Depends on Ace2 and Tmprss2 and Is Blocked by a Clinically Proven Protease Inhibitor." *Cell* 181, no. 2 (Apr 16 2020): 271-80 e8. <https://doi.org/10.1016/j.cell.2020.02.052>.  
<https://www.ncbi.nlm.nih.gov/pubmed/32142651>.
  15. Hu, B., H. Guo, P. Zhou, and Z. L. Shi. "Characteristics of Sars-Cov-2 and Covid-19." *Nat Rev Microbiol* (Oct 6 2020). <https://doi.org/10.1038/s41579-020-00459-7>.  
<https://www.ncbi.nlm.nih.gov/pubmed/33024307>.
  16. Huang, C., K. G. Lokugamage, J. M. Rozovics, K. Narayanan, B. L. Semler, and S. Makino. "Sars Coronavirus Nsp1 Protein Induces Template-Dependent Endonucleolytic Cleavage of Mrnas: Viral Mrnas Are Resistant to Nsp1-Induced Rna Cleavage." *PLoS Pathog* 7, no. 12 (Dec 2011): e1002433.  
<https://doi.org/10.1371/journal.ppat.1002433>.  
<https://www.ncbi.nlm.nih.gov/pubmed/22174690>.
  17. Islam, M. R., M. N. Hoque, M. S. Rahman, Asmru Alam, M. Akther, J. A. Puspo, S. Akter, *et al.* "Genome-Wide Analysis of Sars-Cov-2 Virus Strains Circulating Worldwide Implicates Heterogeneity." *Sci Rep* 10, no. 1 (Aug 19 2020): 14004.  
<https://doi.org/10.1038/s41598-020-70812-6>.  
<https://www.ncbi.nlm.nih.gov/pubmed/32814791>.
  18. Islek, A., and M. K. Balci. "Diagnostic Value of Butanol Threshold Test in Covid-19 Related Olfactory Dysfunction." *Indian J Otolaryngol Head Neck Surg* (Feb 6 2021): 1-5. <https://doi.org/10.1007/s12070-021-02420-3>.  
<https://www.ncbi.nlm.nih.gov/pubmed/33585176>.
  19. Johnson-Leon, M., A. L. Caplan, L. Kenny, I. Buchan, L. Fesi, P. Olhava, D. Nsobila Alugnoa, *et al.* "Executive Summary: It's Wrong Not to Test: The Case for Universal, Frequent Rapid Covid-19 Testing." *EClinicalMedicine* (Feb 19 2021): 100759. <https://doi.org/10.1016/j.eclinm.2021.100759>.  
<https://www.ncbi.nlm.nih.gov/pubmed/33644720>.
  20. Karki, R., B. R. Sharma, S. Tuladhar, E. P. Williams, L. Zalduondo, P. Samir, M. Zheng, *et al.* "Synergism of Tnf-Alpha and Ifn-Gamma Triggers Inflammatory Cell Death, Tissue Damage, and Mortality in Sars-Cov-2 Infection and Cytokine Shock Syndromes." *Cell* 184, no. 1 (Jan 7 2021): 149-68 e17.  
<https://doi.org/10.1016/j.cell.2020.11.025>.  
<https://www.ncbi.nlm.nih.gov/pubmed/33278357>.

21. Kellogg, D. E., I. Rybalkin, S. Chen, N. Mukhamedova, T. Vlasik, P. D. Siebert, and A. Chenchik. "Taqstart Antibody: "Hot Start" Pcr Facilitated by a Neutralizing Monoclonal Antibody Directed against Taq DNA Polymerase." *Biotechniques* 16, no. 6 (Jun 1994): 1134-7. <https://www.ncbi.nlm.nih.gov/pubmed/8074881>.
22. Kiewiet, M. G., J. Grundstrom, D. Apostolovic, M. Andersson, M. P. Borres, C. Hamsten, M. Starkhammar, and M. van Hage. "Elucidating the Alpha-Gal Syndrome at the Molecular Allergen Level." *Allergy* (Nov 18 2020). <https://doi.org/10.1111/all.14660>.  
<https://www.ncbi.nlm.nih.gov/pubmed/33206401>.
23. Kilic, A., B. Hiestand, and E. Palavecino. "Evaluation of Performance of the Bd Veritor Sars-Cov-2 Chromatographic Immunoassay Test in Covid-19 Symptomatic Patients." *J Clin Microbiol* (Feb 26 2021). <https://doi.org/10.1128/JCM.00260-21>.  
<https://www.ncbi.nlm.nih.gov/pubmed/33637583>.
24. Klenow, H., and I. Henningsen. "Selective Elimination of the Exonuclease Activity of the Deoxyribonucleic Acid Polymerase from Escherichia Coli B by Limited Proteolysis." *Proc Natl Acad Sci U S A* 65, no. 1 (Jan 1970): 168-75. <https://doi.org/10.1073/pnas.65.1.168>.  
<https://www.ncbi.nlm.nih.gov/pubmed/4905667>.
25. Kralik, P., and M. Ricchi. "A Basic Guide to Real Time Pcr in Microbial Diagnostics: Definitions, Parameters, and Everything." *Front Microbiol* 8 (2017): 108. <https://doi.org/10.3389/fmicb.2017.00108>.  
<https://www.ncbi.nlm.nih.gov/pubmed/28210243>.
26. Langer, A., M. Schraml, R. Strasser, H. Daub, T. Myers, D. Heindl, and U. Rant. "Polymerase/DNA Interactions and Enzymatic Activity: Multi-Parameter Analysis with Electro-Switchable Biosurfaces." *Sci Rep* 5 (Jul 15 2015): 12066. <https://doi.org/10.1038/srep12066>.  
<https://www.ncbi.nlm.nih.gov/pubmed/26174478>.
27. Lawyer, F. C., S. Stoffel, R. K. Saiki, S. Y. Chang, P. A. Landre, R. D. Abramson, and D. H. Gelfand. "High-Level Expression, Purification, and Enzymatic Characterization of Full-Length Thermus Aquaticus DNA Polymerase and a Truncated Form Deficient in 5' to 3' Exonuclease Activity." *PCR Methods Appl* 2, no. 4 (May 1993): 275-87. <https://doi.org/10.1101/gr.2.4.275>.  
<https://www.ncbi.nlm.nih.gov/pubmed/8324500>.
28. Liu, C. C., and V. J. LiCata. "The Stability of Taq DNA Polymerase Results from a Reduced Entropic Folding Penalty; Identification of Other Thermophilic Proteins with Similar Folding Thermodynamics." *Proteins* 82, no. 5 (May 2014): 785-93. <https://doi.org/10.1002/prot.24458>.  
<https://www.ncbi.nlm.nih.gov/pubmed/24174290>.
29. Lu, R., X. Zhao, J. Li, P. Niu, B. Yang, H. Wu, W. Wang, *et al.* "Genomic Characterisation and Epidemiology of 2019 Novel Coronavirus: Implications for Virus Origins and Receptor Binding." *Lancet* 395, no. 10224 (Feb 22 2020): 565-74. [https://doi.org/10.1016/S0140-6736\(20\)30251-8](https://doi.org/10.1016/S0140-6736(20)30251-8).  
<https://www.ncbi.nlm.nih.gov/pubmed/32007145>.
30. Mancini, F., F. Barbanti, M. Scaturro, S. Fontana, A. Di Martino, G. Marsili, S. Puzelli, *et al.* "Multiplex Rt-Real Time Pcr Assays for Diagnostic Testing of Sars-



- Cov-2 and Seasonal Influenza Viruses. A Challenge of the Phase 3 Pandemic Setting." *J Infect Dis* (Oct 20 2020). <https://doi.org/10.1093/infdis/jiaa658>.  
<https://www.ncbi.nlm.nih.gov/pubmed/33080031>.
31. Mendels, D. A., L. Dortet, C. Emeraud, S. Oueslati, D. Girlich, J. B. Ronat, S. Bernabeu, *et al.* "Using Artificial Intelligence to Improve Covid-19 Rapid Diagnostic Test Result Interpretation." *Proc Natl Acad Sci U S A* 118, no. 12 (Mar 23 2021). <https://doi.org/10.1073/pnas.2019893118>.  
<https://www.ncbi.nlm.nih.gov/pubmed/33674422>.
  32. Millington, A. L., J. A. Houskeeper, J. F. Quackenbush, J. M. Trauba, and C. T. Wittwer. "The Kinetic Requirements of Extreme Qpcr." *Biomol Detect Quantif* 17 (Mar 2019): 100081. <https://doi.org/10.1016/j.bdq.2019.100081>.  
<https://www.ncbi.nlm.nih.gov/pubmed/31285997>.
  33. Mullis, K. B. "Target Amplification for DNA Analysis by the Polymerase Chain Reaction." *Ann Biol Clin (Paris)* 48, no. 8 (1990): 579-82.  
<https://www.ncbi.nlm.nih.gov/pubmed/2288446>.
  34. ———. "The Unusual Origin of the Polymerase Chain Reaction." *Sci Am* 262, no. 4 (Apr 1990): 56-61, 64-5. <https://doi.org/10.1038/scientificamerican0490-56>.  
<https://www.ncbi.nlm.nih.gov/pubmed/2315679>.
  35. Myrick, J. T., R. J. Pryor, R. A. Palais, S. J. Ison, L. Sanford, Z. L. Dwight, J. J. Huuskonen, S. O. Sundberg, and C. T. Wittwer. "Integrated Extreme Real-Time Pcr and High-Speed Melting Analysis in 52 to 87 Seconds." *Clin Chem* 65, no. 2 (Feb 2019): 263-71. <https://doi.org/10.1373/clinchem.2018.296608>.  
<https://www.ncbi.nlm.nih.gov/pubmed/30459167>.
  36. Nguyen, T. T., T. N. Pham, T. D. Van, T. T. Nguyen, D. T. N. Nguyen, H. N. M. Le, J. S. Eden, *et al.* "Genetic Diversity of Sars-Cov-2 and Clinical, Epidemiological Characteristics of Covid-19 Patients in Hanoi, Vietnam." *PLoS One* 15, no. 11 (2020): e0242537. <https://doi.org/10.1371/journal.pone.0242537>.  
<https://www.ncbi.nlm.nih.gov/pubmed/33201914>.
  37. Palais, R., and C. T. Wittwer. "Mathematical Algorithms for High-Resolution DNA Melting Analysis." *Methods Enzymol* 454 (2009): 323-43.  
[https://doi.org/10.1016/S0076-6879\(08\)03813-5](https://doi.org/10.1016/S0076-6879(08)03813-5).  
<https://www.ncbi.nlm.nih.gov/pubmed/19216933>.
  38. Polack, F. P., S. J. Thomas, N. Kitchin, J. Absalon, A. Gurtman, S. Lockhart, J. L. Perez, *et al.* "Safety and Efficacy of the Bnt162b2 Mrna Covid-19 Vaccine." *N Engl J Med* 383, no. 27 (Dec 31 2020): 2603-15.  
<https://doi.org/10.1056/NEJMoa2034577>.  
<https://www.ncbi.nlm.nih.gov/pubmed/33301246>.
  39. Rejali, N. A., A. M. Zwitter, J. F. Quackenbush, and C. T. Wittwer. "Reverse Transcriptase Kinetics for One-Step Rt-Pcr." *Anal Biochem* 601 (Jul 15 2020): 113768. <https://doi.org/10.1016/j.ab.2020.113768>.  
<https://www.ncbi.nlm.nih.gov/pubmed/32416095>.
  40. Reuveni, S., M. Urbakh, and J. Klafter. "Role of Substrate Unbinding in Michaelis-Menten Enzymatic Reactions." *Proc Natl Acad Sci U S A* 111, no. 12 (Mar 25 2014): 4391-6. <https://doi.org/10.1073/pnas.1318122111>.  
<https://www.ncbi.nlm.nih.gov/pubmed/24616494>.



41. Romano, M., A. Ruggiero, F. Squeglia, G. Maga, and R. Berisio. "A Structural View of Sars-Cov-2 Rna Replication Machinery: Rna Synthesis, Proofreading and Final Capping." *Cells* 9, no. 5 (May 20 2020).  
<https://doi.org/10.3390/cells9051267>.  
<https://www.ncbi.nlm.nih.gov/pubmed/32443810>.
42. Ryabkova, V. A., L. P. Churilov, and Y. Shoenfeld. "Influenza Infection, Sars, Mers and Covid-19: Cytokine Storm - the Common Denominator and the Lessons to Be Learned." *Clin Immunol* 223 (Dec 14 2020): 108652.  
<https://doi.org/10.1016/j.clim.2020.108652>.  
<https://www.ncbi.nlm.nih.gov/pubmed/33333256>.
43. Saiki, R. K., D. H. Gelfand, S. Stoffel, S. J. Scharf, R. Higuchi, G. T. Horn, K. B. Mullis, and H. A. Erlich. "Primer-Directed Enzymatic Amplification of DNA with a Thermostable DNA Polymerase." *Science* 239, no. 4839 (Jan 29 1988): 487-91.  
<https://doi.org/10.1126/science.2448875>.  
<https://www.ncbi.nlm.nih.gov/pubmed/2448875>.
44. Saiki, R. K., S. Scharf, F. Faloona, K. B. Mullis, G. T. Horn, H. A. Erlich, and N. Arnheim. "Enzymatic Amplification of Beta-Globin Genomic Sequences and Restriction Site Analysis for Diagnosis of Sickle Cell Anemia." *Science* 230, no. 4732 (Dec 20 1985): 1350-4. <https://doi.org/10.1126/science.2999980>.  
<https://www.ncbi.nlm.nih.gov/pubmed/2999980>.
45. SantaLucia, J., Jr., and D. Hicks. "The Thermodynamics of DNA Structural Motifs." *Annu Rev Biophys Biomol Struct* 33 (2004): 415-40.  
<https://doi.org/10.1146/annurev.biophys.32.110601.141800>.  
<https://www.ncbi.nlm.nih.gov/pubmed/15139820>.
46. Swain, K. C., and C. Singha. "Low-Cost Technology for Covid-19 Infection Detection through Smell Loss Test: An Overview." *Trop Biomed* 37, no. 3 (Sep 1 2020): 671-82. <https://doi.org/10.47665/tb.37.3.671>.  
<https://www.ncbi.nlm.nih.gov/pubmed/33612781>.
47. Tan, Z. J., and S. J. Chen. "Nucleic Acid Helix Stability: Effects of Salt Concentration, Cation Valence and Size, and Chain Length." *Biophys J* 90, no. 4 (Feb 15 2006): 1175-90. <https://doi.org/10.1529/biophysj.105.070904>.  
<https://www.ncbi.nlm.nih.gov/pubmed/16299077>.
48. Tang, L., Z. Yin, Y. Hu, and H. Mei. "Controlling Cytokine Storm Is Vital in Covid-19." *Front Immunol* 11 (2020): 570993.  
<https://doi.org/10.3389/fimmu.2020.570993>.  
<https://www.ncbi.nlm.nih.gov/pubmed/33329533>.
49. Taylor, S. C., G. Laperriere, and H. Germain. "Droplet Digital Pcr Versus Qpcr for Gene Expression Analysis with Low Abundant Targets: From Variable Nonsense to Publication Quality Data." *Sci Rep* 7, no. 1 (May 25 2017): 2409.  
<https://doi.org/10.1038/s41598-017-02217-x>.  
<https://www.ncbi.nlm.nih.gov/pubmed/28546538>.
50. Thoms, M., R. Buschauer, M. Ameismeier, L. Koepke, T. Denk, M. Hirschenberger, H. Kratzat, *et al.* "Structural Basis for Translational Shutdown and Immune Evasion by the Nsp1 Protein of Sars-Cov-2." *Science* 369, no. 6508 (Sep 4 2020): 1249-55. <https://doi.org/10.1126/science.abc8665>.  
<https://www.ncbi.nlm.nih.gov/pubmed/32680882>.

51. Torres, I., S. Poujois, E. Albert, G. Alvarez, J. Colomina, and D. Navarro. "Point-of-Care Evaluation of a Rapid Antigen Test (Clinitest() Rapid Covid-19 Antigen Test) for Diagnosis of Sars-Cov-2 Infection in Symptomatic and Asymptomatic Individuals." *J Infect* (Feb 12 2021). <https://doi.org/10.1016/j.jinf.2021.02.010>.  
<https://www.ncbi.nlm.nih.gov/pubmed/33587922>.
52. Vologodskii, A., and M. D. Frank-Kamenetskii. "DNA Melting and Energetics of the Double Helix." *Phys Life Rev* 25 (Aug 2018): 1-21.  
<https://doi.org/10.1016/j.plrev.2017.11.012>.  
<https://www.ncbi.nlm.nih.gov/pubmed/29170011>.
53. Wadhwa, A., A. Aljabbari, A. Lokras, C. Foged, and A. Thakur. "Opportunities and Challenges in the Delivery of Mrna-Based Vaccines." *Pharmaceutics* 12, no. 2 (Jan 28 2020). <https://doi.org/10.3390/pharmaceutics12020102>.  
<https://www.ncbi.nlm.nih.gov/pubmed/32013049>.
54. Walls, A. C., Y. J. Park, M. A. Tortorici, A. Wall, A. T. McGuire, and D. Veessler. "Structure, Function, and Antigenicity of the Sars-Cov-2 Spike Glycoprotein." *Cell* 183, no. 6 (Dec 10 2020): 1735. <https://doi.org/10.1016/j.cell.2020.11.032>.  
<https://www.ncbi.nlm.nih.gov/pubmed/33306958>.
55. Wang, D., B. Hu, C. Hu, F. Zhu, X. Liu, J. Zhang, B. Wang, *et al.* "Clinical Characteristics of 138 Hospitalized Patients with 2019 Novel Coronavirus-Infected Pneumonia in Wuhan, China." *JAMA* 323, no. 11 (Mar 17 2020): 1061-69. <https://doi.org/10.1001/jama.2020.1585>.  
<https://www.ncbi.nlm.nih.gov/pubmed/32031570>.
56. Xia, S., Y. Zhu, M. Liu, Q. Lan, W. Xu, Y. Wu, T. Ying, *et al.* "Fusion Mechanism of 2019-Ncov and Fusion Inhibitors Targeting Hr1 Domain in Spike Protein." *Cell Mol Immunol* 17, no. 7 (Jul 2020): 765-67. <https://doi.org/10.1038/s41423-020-0374-2>.  
<https://www.ncbi.nlm.nih.gov/pubmed/32047258>.

## VITA

Grayson Welch Way was born on March 2<sup>nd</sup>, 1989, in Henrico County, Virginia and is an American Citizen. He graduated from St. Christopher's High School in Richmond, Virginia in 2007. He received his Bachelor of Science from James Madison University, Harrisonburg, Virginia in 2011.